Acta Materialia 107 (2016) 127–132

Contents lists available at ScienceDirect

Acta Materialia

journal homepage: www.elsevier.com/locate/actamat

Full length article

Contribution of van der Waals forces to the plasticity of magnesium

Zhigang Ding [a], Wei Liu [a, *], Shuang Li [a], Dalong Zhang [b], Yonghao Zhao [a], Enrique J. Lavernia [b], Yuntian Zhu [a, c]

[a] Nano Structural Materials Center, School of Materials Science and Engineering, Nanjing University of Science and Technology, Nanjing, Jiangsu 210094, China
[b] Engineering and Materials Science, University of California, Irvine, CA 92697-1000, USA
[c] Department of Materials Science and Engineering, North Carolina State University, Raleigh, NC 27695, USA

ARTICLE INFO

Article history:
Received 6 November 2015
Received in revised form
5 January 2016
Accepted 10 January 2016
Available online 5 February 2016

Keywords:
Magnesium
Generalized stacking fault energy
Restoring stress
Density-functional theory
van der Waals forces

ABSTRACT

The accurate determination of stacking fault energies (SFE) and associated restoring forces is important for understanding plastic deformation, especially the dislocation emission and motion in metals. In this work, we use density-functional theory (DFT) calculations to, systematically study the all-dimension relaxed atomic models of Mg crystal slip, with a special focus on the "subslip modes" in prismatic and pyramidal slip systems. We find that slip systems with large interplanar distances are readily activated, which agrees well with experimental observations. Inclusion of the ubiquitous van der Waals (vdW) interactions results in lower generalized stacking fault energy curves. Remarkably, the unstable SFE value of pyramidal-II system is strongly reduced by up to 69 mJ/m^2, and the related restoring stress is lowered by 0.74 GPa after taking into account the vdW energy. Our calculations indicate significant effect of vdW forces on the plasticity of Mg.

1. Introduction

Magnesium (Mg) and its alloys have found extensive applications in automobile, aircraft, and electronic components, due to their high strength, lightweight, and good electric properties [1,2]. However, their broader applications in modern industry are severely limited by their low tensile strength and poor plasticity [3–5]. Typically, the plastic deformation in Mg is primarily carried out by five slip systems on basal, prismatic and pyramidal planes. Facilitating cross slip from basal plane to prismatic and pyramidal planes has been shown as a promising method to enhance the plasticity of hcp metals. Unlike the basal plane in Fig. 1a, the interplanar distances are not identical in prismatic and pyramidal planes, leading to two slip systems (named as type "I" and type "II") along the same $<11\bar{2}0>$ direction (Fig. 1b and c). Although such "subslip phenomenon" generally exists in hcp metals [6], it was often neglected in previous studies. As such, one would cast doubt on the sufficiency of slip systems normally defined in hcp crystals, raising a question on the most preferable slip route for Mg. In addition, due to the anisotropic deformation behavior and the lack of easy-slip systems in hcp metals, deformation mechanisms of Mg and its alloys are known to be more complicated than their face-centered and body-centered cubic counterparts [7–9].

The stacking fault energy (SFE) is a key parameter for understanding the deformation mechanism of metals. The SFE value represents the energy associated with interrupting the normal stacking sequence of a crystal plane, and significantly affects the mobility of dislocations. To interpret the mobility of dislocations, the generalized stacking fault energy (GSFE) curve is often calculated, which involves both stable and unstable SFEs. Obviously, an accurate GSFE curve is important, both for determining the energy barrier between two adjacent planes in a slip system, and for calculating the restoring force described in the famous Peierls-Nabarro model for dislocations [10,11]. However, there is a large scatter in the SFE data obtained from experiments. For example, the SFE values for pure Mg range from 50 to 280 mJ/m^2 [12–14]. The large discrepancy in determining the SFE values reflects the difficulty in finding the correct slip modes and resulting deformation mechanisms in Mg.

Density-functional theory (DFT) calculations are widely used to calculate the SFE and GSFE curves. For example, Smith [15] has used generalized gradient approximation (GGA) method to study four different basal plane stable SFEs, and the unstable SFEs on basal, prismatic, and pyramidal planes. He found that the unstable SFE of

* Corresponding author.
E-mail address: weiliu@njust.edu.cn (W. Liu).

http://dx.doi.org/10.1016/j.actamat.2016.01.026
1359-6454/

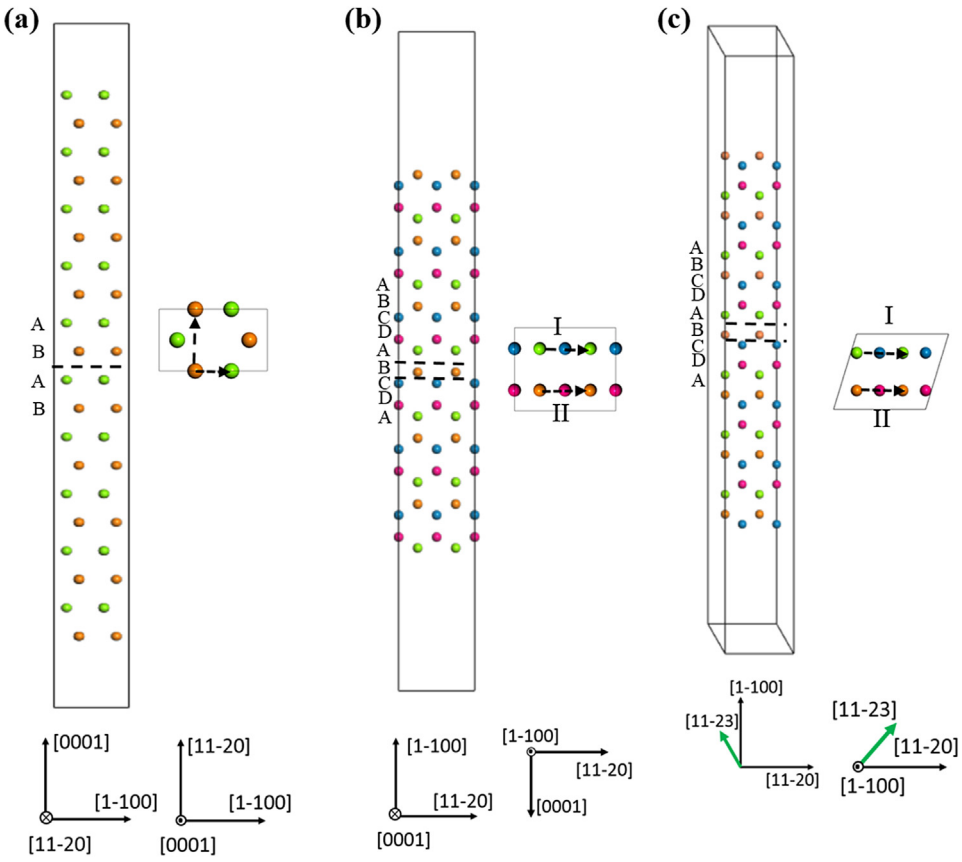

Fig. 1. The slab supercells used to calculate the GSFE of magnesium for basal plane (a), prismatic plane (b), and pyramidal plane (c). In plot (a), the dotted line in the side view represents the slip plane, and the arrows in the top view denote the $<1\bar{1}00>$ and $<11\bar{2}0>$ slip directions. In plots (b) and (c), there exist two slip planes in the prismatic and pyramidal planes due to the difference in interplanar distances. Slip along AB layer with a large distance is named as "I", slip along BC layer with a small distance is named as "II". The arrows in the top views indicate the two slip modes.

the pyramidal plane is 30% greater than that on the prismatic plane, and the SFE results from GGA are consistently lower than those from the local-density approximation (LDA) method. Also using the GGA method, Wen *et al.* [16] systematically calculated the GSFE surface of basal planes and non-basal planes, concluding that slip occurs primarily on basal plane for pure Mg. These DFT calculations provide insights into the underlying deformation mechanisms of Mg. However, it is known that the standard DFT functionals, including both LDA and GGA, cannot capture the long-range van der Waals (vdW) interactions for nonhomogeneous electron densities [17,18]. This may lead to serious errors in the prediction of the structure, stability, and function of materials [19–22]. A recent work has clearly demonstrated that the inclusion of vdW interactions is necessary for obtaining reasonable structures observed from experiments for noble metals and alkali metal [23]. In addition, vdW forces are found to make considerable contribution to the stability and cohesive properties, such as cohesive energies and bulk moduli, of metals [24]. Notably, many previous studies have focused on the role of vdW interactions in *alkaline-earth metal clusters* [25–28]. A consensus from all these studies is that the vdW interactions play a critical role in alkaline-earth metal clusters, including Mg, and the inclusion of the vdW in the calculation yields better agreement with available experimental data. For example, the vdW interactions can significantly reduce the binding energy of Mg dimer from 3.28 to 1.39 kcal/mol, making it much closer to the experimental data (1.21 kcal/mol) [25]. Although the effects of vdW forces have been reported in bulk metals such as Cu, Al, Ag, and Au [29], their contributions to mechanical properties of Mg bulk have yet to be explored. Therefore, one would expect the vdW forces to affect the SFE values and GSFE curves. However, no previous studies have considered the role of vdW forces in metal plasticity.

In this contribution, we systematically study the slip modes and plasticity of hcp Mg by including the vdW effects in the DFT calculation. We find that the inclusion of vdW interactions consistently results in lower SFE values than those from the standard GGA-PBE functional. In particular, vdW interactions are found to contribute more to unstable SFEs than to stable ones, due to the different degree of charge density distributions in the two systems. We also find that the slip along a plane with a larger interplanar distance is easier to be activated in prismatic and pyramidal planes, which is consistent with experimental findings. Our results would help with understanding the cross slip from basal plane to non-basal planes, and the resulting plastic deformation mechanism in hcp metals.

2. Computation approach

All calculations were performed using the Vienna Ab-initio Simulation Package (VASP) [30]. The interaction between the valence electrons and ionic cores was described by the projector augmented wave (PAW) method [31]. The standard Perdew–Burke–Ernzerhof (PBE) form of the GGA [32] was used as the exchange-correlation functional throughout the paper. A vdW-inclusive approach named optB88-vdW [29,33] was employed to account for dispersion interactions in our calculations. The optB88-

vdW functional is a modified version of the original vdW-DF functional of Dion [34]. By using an empirically optimized optB88-like exchange functional, the optB88-vdW method can accurately describe intermolecular interactions with mean absolute errors on the order of 9% [33,35]. In addition, the mean error for lattice constants is merely 0.012 Å from optB88-vdW, which is significantly smaller than that from the standard PBE functional (0.105 Å). Similarly, the relative error of atomization energies is −1.3% from optB88-vdW and −4.4% from PBE [29]. Thus one would expect that the optB88-vdW functional should also be reasonably good for the Mg systems studied in the present work.

For Mg bulk lattice constant calculations, the Brillouin zone was sampled with a 16 × 16 × 16 *k*-point mesh, and the energy cutoff was set to 400 eV. The geometry optimizations were carried out for the Mg bulk crystal in the hcp structure employing GGA-PBE and optB88-vdW methods. As shown in Table 1, the PBE method predicts the lattice constant *a* of 3.193 Å and *c* of 5.184 Å, which were in agreement with experimental values [36]. The lattice constant agrees even better with experiments with optB88-vdW method when compared to PBE calculations. Using the lattice constant from the optB88-vdW method, we built 20-layer slabs with a (1 × 1) unit cell to represent the basal plane stacking fault structure (see Fig. 1a). Similarly, the prismatic and pyramidal plane stacking fault structures were represented by 24-layer (48 atoms; Fig. 1b) and 26-layer slabs (52 atoms; Fig. 1c), respectively. Each slab was separated by at least 20 Å vacuum to eliminate artificial interactions between the slabs. For slab calculations, the Brillouin zone was sampled with a 18 × 20 × 2 *k*-point mesh, along with an energy cutoff 400 eV. Finally, a residual force threshold of 0.001 eV/A was used for geometry optimizations. The convergence tests show that the error bar of the total energy was less than 0.1 meV/atom when more accurate parameters were used in our computations. As to the GSFE curve calculation we used conventional direct crystal slip technique, in which all atoms were relaxed only in directions perpendicular to the glide planes and displacements of the crystal half part along the direct slip path were constants.

3. Results and discussion

We start with determining the SFE values of stable structures. The conventional definition of SFE is based on the surface tension and repulsion forces between the boundaries of fault region caused by partial dislocation. For Mg, the basal plane is the typical slip plane that has the densest surface and four stacking fault structures, normally termed as I_1, I_2, E, and T_2. Starting from ideal hcp stacking sequence … ABAB …, the intrinsic fault, I_1, is formed by removing an A plane above the B plane, followed by slipping the crystal above this fault of $\frac{1}{3}<1\bar{1}00>$. For the I_1 structure, we find that PBE and optB88-vdW give almost the same SFE data (18 and 17 mJ/m^2; Table 2), and both results are consistent with previous DFT-GGA studies (18 and 16 mJ/m^2) [15,16].

The same conclusion, *i.e.*, the PBE and optB88-vdW functionals provide the same SFE values, can also be achieved in the I_2, E, and T_2 systems (*c.f.* Table 2). The deformation fault, or the intrinsic fault, I_2, is formed by direct slip along $\frac{1}{3}<1\bar{1}00>$ direction. The extrinsic stacking fault (E) generated by inserting an extra C plane into the hcp structure. Remarkably, Table 2 shows that the SFE values of I_2 and E are nearly twice and triple of I_1, which was attributed to the variation of local environment of atoms [37]. Specifically, there are one fcc-like environment atom (*i.e.* ABC stacking sequence) in I_1, two in I_2, and three in E. Therefore, the SFE follows the rule that $\gamma_E = 3/2\gamma_{I_2} = 3\gamma_{I_1}$. Although basal plane is the most frequently observed slip plane in Mg, it does not correspond to a twin. The twinlike stacking fault, T_2, was named by its mirror symmetry structure. Although the T_2 structure also possesses two fcc-like environment atoms, the calculated results are slightly larger than that of I_2. This distinction was expected to originate from the different next-nearest neighbor coordinates [38].

Table 1
Equilibrium lattice constant and the c/a ratio of Mg crystal from different methods. The available experimental values are also listed for comparison [36].

Method	a (Å)	c (Å)	c/a
PBE	3.193	5.184	1.624
optB88-vdW	3.198	5.184	1.624
Experiment	3.209	5.210	1.624

Table 2
Stacking sequences and SFEs values (in mJ/m^2) of growth fault (intrinsic fault I_1), deformation fault (intrinsic fault I_2), extrinsic fault (E) and twinlike fault (T_2) structures in hcp Mg by PBE and optB88-vdW methods.

System	Stacking sequence	PBE	optB88-vdW	PBE [15]	PW91 [16]
I_1	ABABABCBCBCB	18	17	18	16
I_2	ABABABCACACA	37	35	36	34
T_2	ABABABCBABAB	40	38	40	36
E	ABABABCABABA	57	56	58	59

To analyze the dislocation core and detect deformation behavior, we now turn to the GSFE curve that provides important information on the unstable SFE and slip process. Fig. 2a and b illustrate the GSFEs for the basal plane as a function of the fault vector u for $\{0001\}<1\bar{1}00>$ and $\{0001\}<11\bar{2}0>$ slip systems, respectively. The unstable SFE corresponds to the maximum energy on the curve. The energy value at the final positions of $\frac{1}{3}<1\bar{1}00>$ corresponds to the intrinsic stable stacking fault I_2 configuration, where a full dislocation dissociates into two Shockley partial dislocations. An analysis of the GSFE curves reveals that although PBE and optB88-vdW give similar stable SFE values, the vdW interactions lead to larger difference in unstable SFE values. As shown in Fig. 2b, unstable SFE along the $<11\bar{2}0>$ direction decreases from 269 mJ/m^2 by PBE to 254 mJ/m^2 by optB88-vdW. The corresponding values of $\frac{1}{3}<1\bar{1}00>$ also decrease at the same ratio.

Fig. 2 also shows the vdW energy versus displacement for basal planes. The vdW energy curve was obtained by decomposing the total optB88-vdW SFE values into the local and non-local correlation (vdW) contributions. The vdW energy along the slip direction shows a parabolic-like curve with the maximum value appears at the unstable position. This demonstrates that the vdW interactions mainly contribute to the unstable stacking fault configuration. We explain this finding by comparing the difference of charge density distributions obtained from the PBE and optB88-vdW methods. As illustrated in Fig. 2c, the red color denotes the area with higher charge density. Our calculations show that atoms further away from the slip plane are surrounded by three regular high charge density areas (labeled A in Fig. 2c). The next-nearest atoms also have three high charge density areas, but the shape of one A area of optB88-vdW have changed to B. The nearest atoms of optB88-vdW have one A area, whilst there are two from PBE. For atoms in the faulted plane, the A area all disappeared in optB88-vdW method. Additionally, the corresponding contour lines of optB88-vdW are larger than that of PBE. We thus conclude that there is more charge transfer in optB88-vdW method and the decrease of unstable SFE is mainly due to modification of charge distribution from slip plane atoms to the next-nearest plane atoms.

We now discuss the energetics for non-basal slip systems, which also play an important role in the deformation process. For these systems we consider two types of interplanar distance for the slip along $\frac{1}{3}<11\bar{2}0>$ direction (see Fig. 1b and c). As shown in Fig. 3, the type II unstable SFE is twice as large as that of type I for prismatic

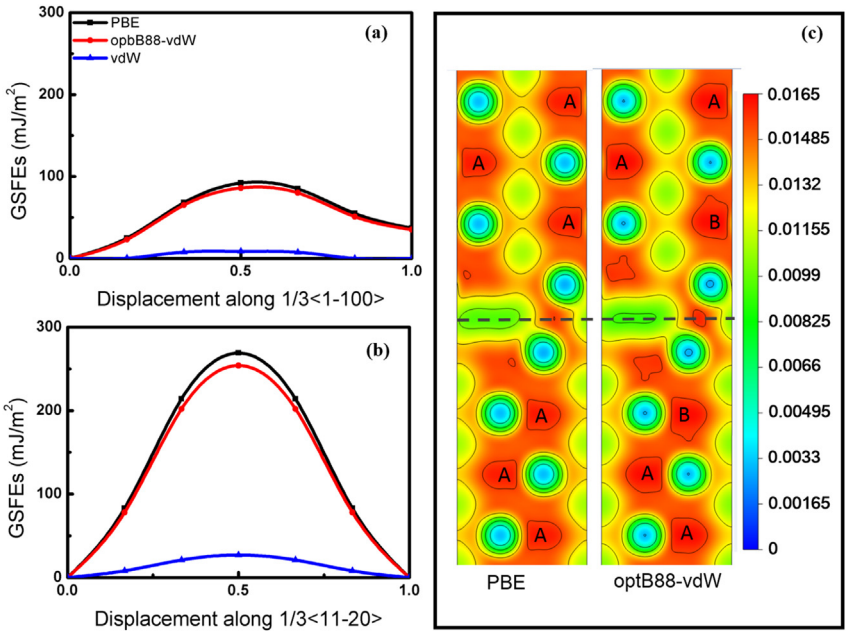

Fig. 2. The GSFE curve of basal plane by PBE and optB88-vdW methods as a function of displacement along (a) $<1\bar{1}00>$ and (b) $<11\bar{2}0>$ directions. The maximum of the curves corresponds to the unstable SFEs. (c) The distributions of charge densities on the unstable position of $<11\bar{2}0>$ direction by PBE and optB88-vdW methods at $\{10\bar{1}0\}$ plane, where red represents high charge density area. Contour lines are drawn at a constant interval, and slip plane is marked by dotted line.

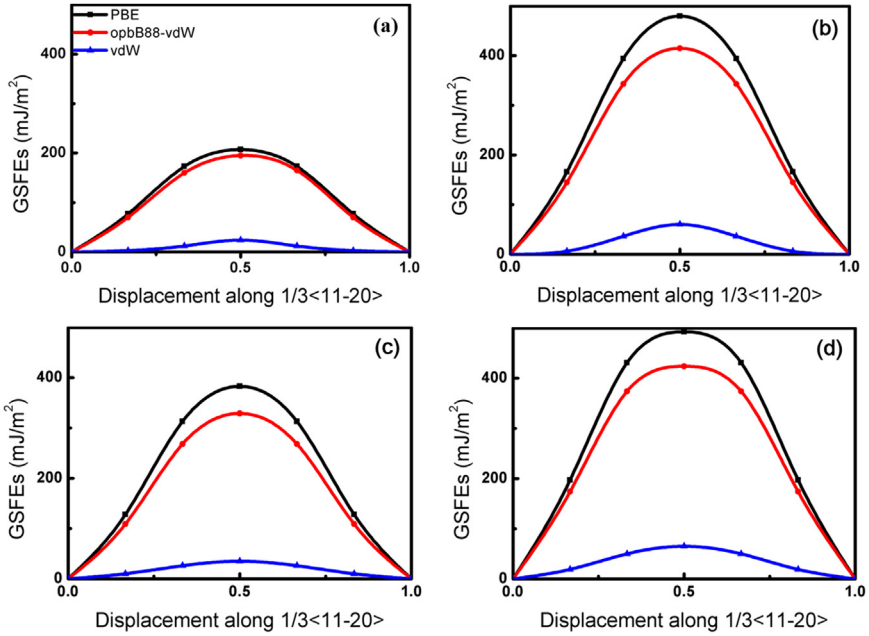

Fig. 3. The GSFE curve of prismatic I (a) and II (b), pyramidal I (c) and II (d) by PBE and optB88-vdW methods as a function of displacement along <11−20> direction. The unstable stacking fault occurs at the displacement of 0.5u.

slip. Similarly, for pyramidal slip the type II unstable SFE is 30% higher compared to that of type I. This result indicates that slip along type I is more readily to be activated than type II, which is consistent with experiments. Clearly, the vdW energy contributes significantly to the unstable stacking fault configurations for both prismatic and pyramidal systems. More importantly, the vdW energy is found to play a more prominent role for the prismatic type II and pyramidal (15% reduction in the unstable SFE value) than for the basal and prismatic type I (6% reduction). This finding is remarkable since it suggests that upon inclusion of the vdW correction, cross slip from basal and prismatic to pyramidal planes becomes easier, which makes the realization of type II possible.

The GSFE curves can also affect the mobility of dislocations. In fact, the core structure of a dislocation can be obtained by solving the corresponding P−N equation at a given restoring force, *f*. In order to obtain an analytical solution of P−N equation, the original P−N model assumed a sinusoidal restoring force:

$$f(u) = \frac{\mu a}{2\pi d} \sin \frac{2\pi u}{a}, \quad (1)$$

where μ, a, and d denote the shear modulus, lattice constant, and interplanar distance, respectively. However, this approximation is crude since the dislocation cores are affected more by the value of the restoring forces at large displacements than in small displacement. In fact, it is shown in Fig. 4 that the restoring force curves do not actually show a sinusoidal behavior. Therefore, finding a more suitable form for restoring force would help with understanding of the dissociated dislocation in Mg.

In 1968, Vitek [39–41] solved the equation numerically by describing the restoring force by the gradient of the GSFE curve,

$$f = -\nabla\gamma(u). \quad (2)$$

Fig. 4 shows the restoring forces for all slip systems. For PBE calculations, the maximum restoring forces of the $\{0001\}<11\bar{2}0>$ slip modes is determined to be 2.59 GPa, which agree well with previous DFT calculations (2.49 GPa) [42]. Upon inclusion of the vdW interactions the restoring force decreased by 0.14 GPa. More remarkably, the restoring force of pyramidal II slip systems is significantly lowered by up to 0.74 GPa, which clearly demonstrates the crucial role of vdW in the determination of mechanical properties in such systems.

Finally, we focus on the contributions of vdW forces to the plasticity of Mg. According to the concept of plasticity of materials in terms of dislocation emission proposed by Rice and Thomson [43], Waghmare et al. [44] defined the disembrittlement parameter D,

$$D = \frac{\gamma_s}{\gamma_{us}} \quad (3)$$

to describe the plasticity of solids, where γ_s is the surface energy, which is defined by the difference between the total energy of the slab including surfaces and a bulk supercell with the same atoms, γ_{us} is unstable SFE. This definition has already been applied to many systems. For example, by using the D parameter, Waghmare *et al.* [44] concluded that the brittleness of $MoSi_2$ would be increased by substitution of Ge or P for Si and Re for Mo. Similarly, Wu *et al.* [45] used the D values to find that the plasticity of Mg can be increased by adding C, N, B, O, and vacancies. Here, the total energy of bulk supercell is obtained from curve fitting by the energy versus the thickness of supercell. For Mg, the surface energy of basal plane calculated by PBE is 550 mJ/m^2, which is consistent with the results from Wu et al. (578 mJ/m^2) [45]. Note that a larger D value indicates increased plasticity, and vice versa. The γ_s value from optB88-vdW is 44 mJ/m^2 larger than that from PBE, leading to a significantly larger D value compared to the PBE (2.3 vs. 2.0). This further confirms that vdW forces may contribute significantly to the Mg plasticity.

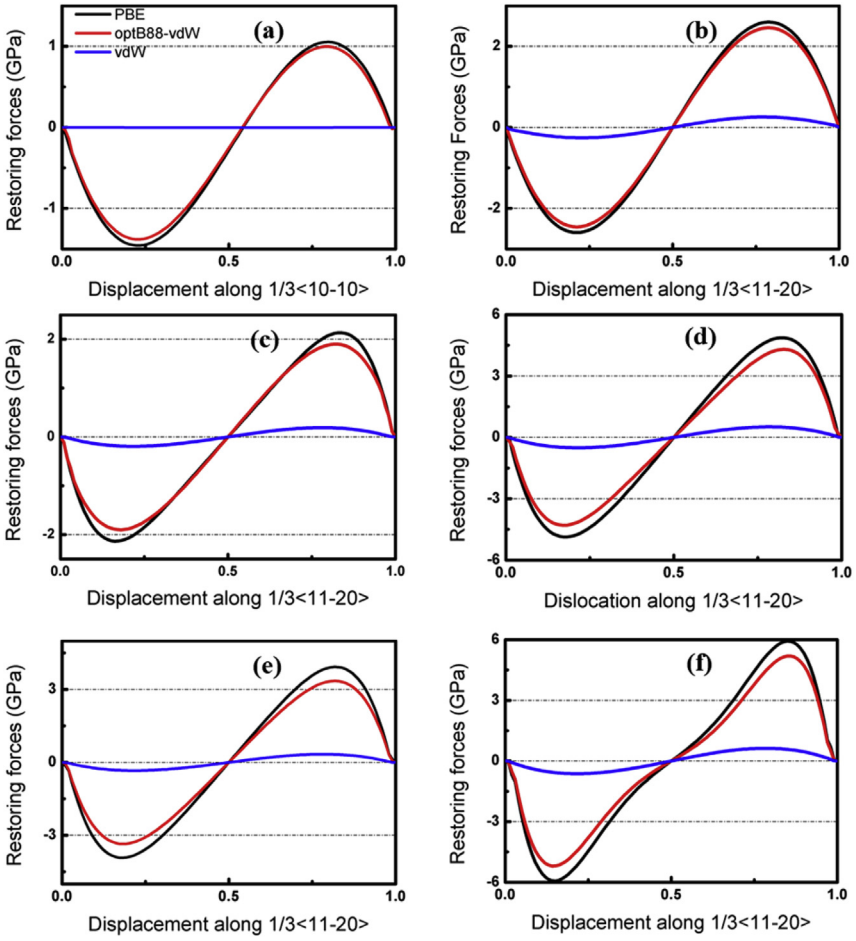

Fig. 4. The restoring forces derived from the negative gradient of GSFE curves of various slip systems: (1) basal plane along $<1\bar{1}00>$ (a) and $<11\bar{2}0>$ (b); (2) prismatic plane I (c) and II (d); (3) pyramidal plane I (e) and II (f).

4. Conclusions

In conclusion, we have carried out DFT calculations to systematically study the slipping mechanism of pure Mg slabs. Our optB88-vdW calculations find that the vdW interactions play a significant role in the slipping process. For the unstable stacking fault configuration of pyramidal-II, inclusion of the vdW reduced the SFE value strongly by up to 69 mJ/m^2, and the related restoring stress may be lowered by up to 0.74 GPa. In addition, the disembrittlement D value increase significantly from 2.0 to 2.3 after considering the vdW interactions, which indicates the prominent role of vdW forces to the Mg plasticity. Our findings indicate the importance of vdW corrections in the accurate prediction of mechanical properties of metals.

Acknowledgments

W.L. and Y.H.Z. are grateful for support from the National Natural Science Foundation of China (nos. 21403113, 51225102, and 2012CB932203), the Natural Science Foundation for Distinguished Young Scholars of Jiangsu Province (no. BK20150035), the Foundation of Jiangsu Specially-Appointed Professor, A Project Funded by the Priority Academic Program Development of Jiangsu Higher Education Institutions, and the Pangu Foundation. Y.T.Z. acknowledges the support of the Jiangsu Key Laboratory of Advanced Micro-Nano Materials and Technology. D.Z. and E.J.L. acknowledge support from NSF-CMMI-1437327.

References

[1] T.M. Pollock, Weight loss with magnesium alloys, Science 328 (2010) 986–987.
[2] H. El Kadiri, A. Oppedal, A crystal plasticity theory for latent hardening by glide twinning through dislocation transmutation and twin accommodation effects, J. Mech. Phys. Solids 58 (2010) 613–624.
[3] K. Lu, L. Lu, S. Suresh, Strengthening materials by engineering coherent internal boundaries at the nanoscale, Science 324 (2009) 349–352.
[4] Y.H. Zhao, Y.T. Zhu, X.Z. Liao, Z. Horita, T.G. Langdon, Tailoring stacking fault energy for high ductility and high strength in ultrafine grained Cu and its alloy, Appl. Phys. Lett. 89 (2006) 121906.
[5] Y.H. Zhao, J. Bingert, Y.T. Zhu, X.Z. Liao, R. Valiev, Z. Horita, T.G. Langdon, Y.Z. Zhou, E.J. Lavernia, Tougher ultrafine grain Cu via high-angle grain boundaries and low dislocation density, Appl. Phys. Lett. 92 (2008) 081903.
[6] P. Kwaśniak, P. Śpiewak, H. Garbacz, K.J. Kurzydlowski, Plasticity of hexagonal systems: split slip modes and inverse Peierls relation in α-Ti, Phys. Rev. B 89 (2014) 144105.
[7] J.A. Yasi, L.G. Hector, D.R. Trinkle, Prediction of thermal cross-slip stress in magnesium alloys from direct first-principles data, Acta Mater. 59 (2011) 5652.
[8] S. Sandlöbes, M. Friak, S. Zaefferer, A. Dick, S. Yi, D. Letzig, Z. Pei, L.-F. Zhu, J. Neugebauer, D. Raabe, The relation between ductility and stacking fault energies in Mg and Mg–Y alloys, Acta Mater. 60 (2012) 3011.
[9] J.P. Hirth, J. Lothe, T. Mura, Theory of Dislocations, second ed., Wiley, New York, 1982.
[10] R. Peierls, The size of a dislocation, Proc. Phys. Soc. 52 (1940) 34–37.
[11] F.R.N. Nabarro, Dislocations in a simple cubic lattice, Proc. Phys. Soc. 59 (1947) 256–272.
[12] D.H. Sastry, Y.V.R.K. Prasad, K.I. Vasu, On the stacking fault energies of some close-packed hexagonal metals, Scr. Metal. 3 (1969) 927.
[13] A. Couret, D. Caillard, An in situ study of prismatic glide in magnesium-II. Microscopic activation parameters, Acta Metal. 33 (1985) 1455–1462.
[14] R.L. Fleischer, Stacking fault energies of HCP metals, Scr. Metal. 20 (1986) 223–224.
[15] A. Smith, Surface, interface and stacking fault energies of magnesium from first principles calculations, Surf. Sci. 601 (2007) 5762–5765.
[16] L. Wen, P. Chen, Z.F. Tong, B.Y. Tang, L.M. Peng, W.J. Ding, A systematic investigation of stacking faults in magnesium via first-principles calculation, Eur. Phys. J. B 72 (2009) 397–403.
[17] A. Tkatchenko, Current understanding of van der Waals effects in realistic materials, Adv. Funct. Mater 25 (2015) 2054–2061.
[18] W. Liu, A. Tkatchenko, M. Scheffer, Modeling adsorption and reactions of organic molecules at metal surfaces, Acc. Chem. Res. 47 (2014) 3369–3377.
[19] J. van Ruitenbeek, Metal/molecule interfaces: dispersion forces unveiled, Nat. Mater. 11 (2012) 834.
[20] W. Liu, A. Savara, X. Ren, W. Ludwig, K.H. Dostert, S. Schauermann, A. Tkatchenko, H.J. Freund, M. Scheffer, Towards low-temperature dehydrogenation catalysis: isophorone on Pd(111), J. Phys. Chem. Lett. 3 (2012) 582.
[21] W. Liu, V.G. Ruiz, G.X. Zhang, B. Santra, X. Ren, M. Scheffler, A. Tkatchenko, Structure and energetics of benzene adsorbed on transition-metal surfaces: density-functional theory with van der Waals interactions including collective substrate response, New J. Phys. 15 (2013) 053046.
[22] W. Liu, J. Carrasco, B. Santra, A. Michaelides, M. Scheffer, A. Tkatchenko, Benzene adsorbed on metals: concerted effect of covalency and van der Waals bonding, Phys. Rev. B 86 (2012) 245405.
[23] J. Carrasco, W. Liu, M. Michaelides, A. Tkatchenko, Insight into the description of van der Waals forces for benzene adsorption on transition metal (111) surfaces, J. Chem. Phys. 140 (2014) 084704.
[24] M.A. Floridia Addato, A.A. Rubert, G.A. Benítez, M.H. Fonticelli, J. Carrasco, P. Carro, R.C. Salvarezza, Alkanethiol adsorption on platinum: chain length effects on the quality of self-assembled monolayers, J. Phys. Chem. C 115 (2011) 17788–17798.
[25] Y. Zhao, D.G. Truhlar, Comparative DFT study of van der Waals complexes: rare-gas dimers, alkaline-earth dimers, zinc dimer, and zinc-rare-gas dimers, J. Phys. Chem. A 110 (2006) 5121–5129.
[26] A. Ruzsinszky, J.P. Perdew, G.I. Csonka, Binding energy curves from nonempirical density functionals II. van der Waals bonds in rare-gas and alkaline-earth diatomics, J. Phys. Chem. A 109 (2005) 11015–11021.
[27] J. Mitroy, M. Bromley, Semiempirical calculation of van der Waals coefficients for alkali-metal and alkaline-earth-metal atoms, Phys. Rev. A 68 (2003) 052714.
[28] A. Swann, J. Ludlow, G. Gribakin, van der Waals coefficients for positronium interactions with atoms, Phys. Rev. A 92 (2015) 012505.
[29] J. Klimeš, D.R. Bowler, A. Michaelides, van der Waals density functionals applied to solids, Phys. Rev. B 83 (2011) 195131.
[30] G. Kresse, J. Furthmüller, Efficiency of ab-initio total energy calculations for metals and semiconductors using a plane-wave basis set, Comput. Mater. Sci. 6 (1996) 15–50.
[31] P.E. Blöchl, Projector augmented-wave method, Phys. Rev. B 50 (1994) 17953.
[32] J.P. Perdew, K. Burke, M. Ernzerhof, Generalized gradient approximation made simple, Phys. Rev. Lett. 77 (1996) 3865.
[33] J. Klimeš, D.R. Bowler, A. Michaelides, Chemical accuracy for the van der Waals density functional, J. Phys. Condens. Matter 22 (2010) 022201.
[34] M. Dion, H. Rydberg, E. Schröder, D.C. Langreth, B.I. Lundqvist, Van der Waals density functional for general geometries, Phys. Rev. Lett. 92 (2004) 246401.
[35] A. Tkatchenko, R.A. DiStasio Jr., R. Car, M. Scheffer, Accurate and efficient method for many-body van der Waals interactions, Phys. Rev. Lett. 108 (2012) 236402.
[36] E. Wachowicz, A. Kiejna, Bulk and surface properties of hexagonal close-packed Be and Mg, J. Phys. Condens. Matter 13 (2001) 10767–10776.
[37] D. Hull, D.J. Bacon, Introduction to Dislocations, Elsevier LTD, Oxford, 2011.
[38] N. Chetty, M. Weinert, Stacking faults in magnesium, Phys. Rev. B 56 (1997) 10844.
[39] V. Vitek, Intrinsic stacking faults in body-centered cubic crystals, Philo. Mag. 18 (1968) 773–786.
[40] K. Ito, V. Vitek, Atomistic study of non-Schmid effects in the plastic yielding of bcc metals, Philo. Mag. A 81 (2001) 1387–1407.
[41] V. Vitek, M. Mrovec, J. Bassani, Influence of non-glide stresses on plastic flow: from atomistic to continuum modeling, Mater. Sci. Eng. A 365 (2004) 31–37.
[42] T.W. Fan, L.G. Luo, L. Ma, B.Y. Tang, L.M. Peng, W.J. Ding, Effects of Zn atoms on the basal dislocation in magnesium solution from Peierls–Nabarro model, Mater. Sci. Eng. A 582 (2013) 299–304.
[43] J.R. Rice, R. Thomson, Ductile versus brittle behaviour of crystals, Philo. Mag. 29 (1974) 73–97.
[44] U. Waghmare, E. Kaxiras, M. Duesbery, Modeling brittle and ductile behavior of solids from first-principles calculations, Phys. Stat. Sol. B 217 (2000) 545–564.
[45] X.Z. Wu, L.L. Liu, R. Wang, L.Y. Gan, Q. Liu, Energy investigations on the mechanical properties of magnesium alloyed by X = C, B, N, O and vacancy, Front. Mater. Sci. 7 (2013) 405–412.